

HOSTED BY



ELSEVIER

Contents lists available at ScienceDirect

Saudi Journal of Biological Sciences

journal homepage: www.sciencedirect.com

Original article

Omega-3 fatty acid-based self-microemulsifying drug delivery system (SMEDDS) of pioglitazone: Optimization, in vitro and in vivo studies

Nasr A. Emad^a, Yasmin Sultana^{a,*}, Mohd Aqil^a, Asmaa Saleh^b, Omkulthom Al kamaly^b, Fahd A Nasr^c^a Department of Pharmaceutics, School of Pharmaceutical Education and Research, Jamia Hamdard (Deemed University), M. B. Road, New Delhi 110062, India^b Department of Pharmaceutical Sciences, College of Pharmacy, Princess Nourah bint Abdulrahman University, P.O Box 84428, Riyadh 11671, Saudi Arabia^c Department of Pharmacognosy, College of Pharmacy, King Saud University, Riyadh, Saudi Arabia

ARTICLE INFO

Article history:

Received 20 March 2023

Revised 2 August 2023

Accepted 10 August 2023

Available online 18 August 2023

Keywords:

Nanoparticles

Pioglitazone

Omega-3 fatty acid

SMEDDS

Insulin resistance

Pharmacokinetics

Central composite design

ABSTRACT

Pioglitazone (PGL) is an effective insulin sensitizer, however, side effects such as accumulation of subcutaneous fat, edema, and weight gain as well as poor oral bioavailability limit its therapeutic potential for oral delivery. Recent studies have shown that combination of both, PGL and fish oil significantly reduce fasting plasma glucose, improve insulin resistance, and mitigate pioglitazone-induced subcutaneous fat accumulation and weight gain. Nevertheless, developing an effective oral drug delivery system for administration of both medications have not been explored yet. Thus, this study aimed to develop a self-micro emulsifying drug delivery system (SMEDDS) for the simultaneous oral administration of PGL and fish oil. SMEDDS was developed using concentrated fish oil, Tween[®] 80, and Transcutol HP and optimized by central composite design (CCD). The reconstituted, optimized PGL-SMEDDS exhibited a globule size of 142 nm, a PDI of 0.232, and a zeta potential of -20.9 mV. The *in-vitro* drug release study of the PGL-SMEDDS showed a first-order model kinetic release and demonstrated remarkable 15-fold enhancement compared to PGL suspension. Additionally, following oral administration in fasting albino Wistar rats, PGL-SMEDDS exhibited 3.4-fold and 1.4-fold enhancements in the AUC_{0-24h} compared to PGL suspension and PGL marketed product. The accelerated stability testing showed that the optimized SMEDDS formulation was stable over a three-month storage period. Taken together, our findings demonstrate that the developed fish oil-based SMEDDS for PGL could serve as effective nanopatforms for the oral delivery of PGL, warranting future studies to explore its synergistic therapeutic potential in rats.

© 2023 The Author(s). Published by Elsevier B.V. on behalf of King Saud University. This is an open access article under the CC BY-NC-ND license (<http://creativecommons.org/licenses/by-nc-nd/4.0/>).

1. Introduction

Impairment in lipid and protein metabolism, as well as hyperglycemia due to abnormalities in insulin production or insulin action, characterise the metabolic disorder known as diabetes mellitus (DM). In the recent decade, diabetes mellitus has risen dra-

matically, especially in undeveloped countries, with more than 641 million people predicted to live with type-2 diabetes worldwide by 2040 (McCormick et al., 2019). Type-2 DM is primarily linked with insulin resistance (IR) due to genetic character, changes in lifestyle, dietary habits, and sedentary behaviours. Blood free fatty acid elevations during hyperglycemic states are associated with decreased insulin gene expression, thus contributing significantly to the pathogenesis of IR in obesity and non-insulin-dependent DM (Amery et al., 2000; Boden, 1996; Kalin et al., 2017). Many approaches for treating diabetes have been reported, ranging from therapeutic approaches (gene therapy, β -cells regeneration, boosting β -cells self-replication, and stem cells) to pharmacological and non-pharmacological approaches (Tan et al., 2019).

Pioglitazone (PGL) belongs chemically to the class of thiazolidinediones, which are selective peroxisome proliferator-activated (PPAR) γ -agonists for the treatment of diabetes type-2. PGL prevents hypoglycemia and preserves β -cell function by decreasing peripheral tissue's IR without inducing insulin produc-

* Corresponding author at: Department of Pharmaceutics, School of Pharmaceutical Education and Research, Jamia Hamdard (Deemed University), M. B. Road, New Delhi 110062, India.

E-mail addresses: nasraliemed_sch@jamiyahamdard.ac.in (N.A. Emad), ysultana@jamiyahamdard.ac.in (Y. Sultana), maqil@jamiyahamdard.ac.in (M. Aqil), AsAli@pnu.edu.sa (A. Saleh), omalkmali@pnu.edu.sa (O. Al kamaly), Fnasr@ksu.edu.sa (F.A Nasr).

Peer review under responsibility of King Saud University.



Production and hosting by Elsevier

<https://doi.org/10.1016/j.sjbs.2023.103778>

1319-562X/© 2023 The Author(s). Published by Elsevier B.V. on behalf of King Saud University.

This is an open access article under the CC BY-NC-ND license (<http://creativecommons.org/licenses/by-nc-nd/4.0/>).

tion (Yajima et al., 2003; Yki-Jarvinen H, 2004). PGL is a Class II medication according to Biopharmaceutical Classification System (BCS), i.e., low solubility (1.8 µg/mL), high permeability, and short half-life (3–6 hr) (Elbary et al., 2008). Whereas PGL is a useful insulin sensitizer, accumulation of subcutaneous fat, weight gain, and edema are considered adverse effects of PGL therapy. In addition, the toxic effects are associated with the dose, and duration of PGL use and could even lead to bladder cancer (Adil et al., 2018; Azoulay et al., 2012; Mamtani et al., 2012; Permanente and California, 2011; Tuccori et al., 2016). Because of this, PGL is now being marketed with some restrictions (Sinha and Ghosal, 2020). Therefore, its poor oral bioavailability and adverse effects impact its therapeutic potential.

EPA and DHA are two examples of polyunsaturated omega-3 fatty acids (PUFAs) rich in fish oil, which is used as a nutritional supplement, that favorably influence plasma lipoproteins and are beneficial to IR and dyslipidemia (Gao et al., 2017; Martins et al., 2018; Yang et al., 2017). The peroxisome proliferator-activated receptor α (PPAR- α) has a mediating role in these actions and omega-3 fatty acids are considered PPAR- α agonists (Eissa et al., 2015; Jump, 2008). PPAR is a nuclear receptor that regulates the transcription of many genes involved in adipocyte differentiation, carbohydrate and lipid metabolism (Varga et al., 2011). The combination of PGL and PUFAs-rich fish oils considerably reduced fasting plasma glucose, improved IR, retarding hepatic lipogenesis, and endoplasmic reticulum stress, therefore inhibiting PGL-induced fat accumulation, weight gain, pancreatic islets hypertrophy, and β -cell dysfunction (Hasan et al., 2020; Iizuka et al., 2018, 2016a, 2016b). However, an effective oral delivery system for both medications have not been developed yet.

SMEDDS are isotropic mixtures of oils and surfactants that generate oil-in-water microemulsions when added to water and stirred gently (Huo et al., 2018). The globule size of the SMEDDS ranges between 50 and 250 nm (Emad et al., 2021). Various researchers reported improved bioavailability of drugs with poor water-solubility after oral administration using SMEDDS (Bolko et al., 2013; Kanwal et al., 2019; Patel and Sawant, 2019; Manali D. Prajapat et al., 2017). Factors such as nano-sized droplets of SMEDDS, higher solubilization capacity, changes in GI tract biochemical barrier function, and lymphatic transport can make a significant contribution to drug absorption (Patel and Sawant, 2019; Manali D Prajapat et al., 2017).

Given the previously described benefits of PGL and omega-3 fatty acids in mitigating insulin resistance. The present work aims to develop and statistically optimize omega-3 fatty acids-based SMEDDS of PGL to enhance its solubility and oral bioavailability. The developed SMEDDS was optimized by using central composite design and evaluated for self-emulsification performance, morphology, stability studies, and *in-vitro* drug release. Furthermore, the *in-vivo* oral bioavailability was compared with that of PGL suspension and PGL marketed product in rats.

2. Materials and methods

2.1. Materials

Sigma-Aldrich, USA was sourced for our supply of PGL (CAS No.: 112529–15–4). Concentrated fish oil (Total Omega-3 Fatty Acids: Minimum 30%) was purchased from Arian Enterprises, Delhi, India. Gift samples of CapryolTM90 and Transcutol[®] HP (UNII code: A1A118X02B) were generously provided by Gattefosse Pvt. Ltd., Mumbai, India. Capmul[®]MCM C8 was obtained from Abetic Corporation, Columbus, USA. Both ethyl oleate and Tween[®] 80 originated from Merck (India). S.D. Fine Chemicals, Ltd. (Mumbai, India) provided us with microcrystalline cellulose, mannitol, soluble starch,

and lactose. The Dialysis tubing membrane was purchased from Abron Exports (Haryana, India). All of the solvents used in the experiments were of analytical quality, and HPLC water was utilised throughout.

2.2. Methods

2.2.1. Screening for SMEDDS components

To choose the appropriate component for SMEDDS, the solubility of pioglitazone HCl was estimated in oils and surfactants. For this, pioglitazone was dissolved in one mL of each vehicle in excess, and the resulting mixtures were vortexed for 15 min to evenly distribute the PGL throughout the vehicles. They were centrifuged at 4000 rpm for 10 min after being incubated at 25 °C in an orbital incubator shaker for 72 hr. Following proper dilution of the supernatant with methanol, the PGL was analyzed spectrometrically by measuring the absorbance at 270 nm (UV-2450, Shimadzu, Japan).

2.2.2. Assessing surfactants emulsification capacity

For screening of the surfactant, a 1:1 (v/v) ratio of the oil phase and surfactant was mixed and diluted fifty times with double distilled water. The % Transmittance and number of inversions were recorded using a UV spectrophotometer at 638 nm (Bolko et al., 2013; Kanwal et al., 2019). Similarly, surfactant and co-surfactant at 2:1 (v/v) were vortexed, diluted fifty times with double distilled water, and the number of inversions and %Transmittance were recorded.

2.2.3. Pseudo-ternary phase diagrams

To develop PGL-SMEDDS, a water titration method was established to estimate the microemulsion region at room temperature. S_{mix} , Tween[®] 80 (surfactant) and Transcutol HP (co-surfactant), were used in four different volume ratios (Km values 1:1, 2:1, 3:1, and 4:1). Different glass vials were used to mix each Km value with increasing percentages of oil by 10th up to 90%, to create the phase diagram. To achieve equilibrium, aliquots of distilled water were slowly added at separate intervals and stirred at 25 °C. The turbid-to-transparent and transparent-to-turbid changes were visually tracked and recorded on a ternary phase diagram table. The free version of CHEMIX was used to construct the pseudo-ternary plots (Manali D. Prajapat et al., 2017).

2.2.4. Optimization of oil and S_{mix}

Design Expert 13 (Stat-Ease Inc., USA) was used to carry out a central composite design (CCD) for the purpose of optimizing the oil and S_{mix} involved in the generation of the SMEDDS. Table 1 summarises both the independent and dependent variables, as well as their respective levels. Globule size, %transmittance, and PDI were optimized as dependent variables, with oil (mg) and S_{mix} (mg) serving as independent variables with varying levels of control over these metrics based on the pseudo-ternary phase diagram result. According to the CCD, there should be 13 formulation runs highlighted on five central points, four factorial points, and four axial points (Alhalmi et al., 2022b).

2.2.5. Preparation of PGL- SMEDDS

Liquid SMEDDS was prepared using a 4:1 S_{mix} ratio based on pseudo-ternary phase diagrams. The oil phase was prepared by mixing fish oil and ethyl oleate (3:1) in screw-capped glass vials using a vortex mixer (Remi, India). The determined amount of S_{mix} was added to the oil phase gradually while stirring constantly until a uniform mixture was obtained. The same steps were used to prepare PGL-loaded SMEDDS. Further, the drug, PGL was dissolved in oil and S_{mix} at a temperature of 50 °C by vortexing and ultrasonication (30 s) to assure the complete dissolution of pioglitazone in SMEDDS (Choi et al., 2014). The amount of pioglitazone was the

Table 1
Variables with levels and constrains used in CCD.

Independent variables	Levels				
	$-\alpha$	-1	0	$+1$	$+\alpha$
Oil (mg) = X1	0.443651	5	16	27	31.5563
S_{mix} (mg) = X2	58.7868	65	80	95	101.213
Dependent Variables	Constraints				
Y1 = droplet size (nm)	Minimum				
Y2 = % transmittance	Maximum				
Y2 = PDI	Minimum				

same in all formulations (7.5 mg/ml SMEDDS). This formulation concentrate was inspected for turbidity, phase separation, or gelling effect and kept at room temperature for further evaluation.

For solid-state characterization, liquid SMEDDS was lyophilized using microcrystalline cellulose (MCC) as a water-soluble carrier. Briefly, 5 % (w/v) of MCC was added to the prepared SMEDDS before it being lyophilized for 6 hr using Bench-top Vacuum Freeze Dryer (FD-10, LABFREEZ INSTRUMENTS GROUP CO., LTD, China).

2.2.6. Evaluation of PGL-SMEDDS

2.2.6.1. %Transmittance and viscosity. A rheometer (Brookfield, Inc., MA, USA), spindle no. 6 at 100 rpm for 5 min, was used to determine the viscosity of pioglitazone-SMEDDS, and the relevant dial reading on the viscometer was recorded. Percent transmittance was determined by diluting the formulation at 10:1000 with double distilled water and measuring the % transmittance at 638 nm by UV-vis spectrophotometer (Patel and Sawant, 2019).

2.2.6.2. Robustness. Robustness to dilution was confirmed by diluting a specific amount of SMEDDS at varied dilution factors (e.g., 50, 100, or 1000 times) with various liquids such as bi-distilled water, 0.1 N HCl, and PBS (pH 7.4). The diluted microemulsions were tested visually at 0, 2, and 6 hr for any physical alteration (Kanwal et al., 2019).

2.2.6.3. Self-emulsification time test. Self-emulsification performance was conducted with a magnetic stirrer running at 200 rpm and distilled water as a medium at 37 ± 0.5 °C. After the addition of one ml of pioglitazone-SMEDDS formulation to 100 ml of the aqueous medium, the time interval between the addition of the SMEDDS and the completion of emulsification, at which point the self-microemulsion was clear and somewhat bluish in appearance, was recorded (Huo et al., 2018).

2.2.6.4. Droplet size, polydispersity index, and zeta potential. The mean globule size, PDI, and zeta potential of the diluted PGL-SMEDDS (1:100 v/v) were determined by Zeta Sizer (Malvern, UK) with the non-invasive backscatter method. Light dispersion due to Brownian droplet motion was measured at a wavelength of 630 nm, a scattering angle of 90°, and a temperature of 25 °C. (Liu et al., 2020).

2.2.6.5. TEM. The transmission electron microscopy (TECHNAI-G2, Netherlands) study was conducted to confirm the morphology of the optimized SMEDDS. A drop of SMEDDS was placed on a grid and left there for one min after being diluted 50 times with bi-distilled water so that it would attach better to the carbon substrate. The grid was then incubated with a drop of 1% phosphotungstate for 10 s, after which the excess solution was filtered off. The material was then dried and examined by transmission electron microscopy (Mohit et al., 2022).

2.2.6.6. Release of PGL-SMEDDS. Using 100 ml of freshly prepared dissolution mediums (0.1 N HCl pH 1.2 and PBS pH 6.8), the in-

vitro release studies were conducted in accordance with the USP XXIV method with some modifications. The apparatus was set at 100 rpm and a temperature of 37 ± 0.5 °C. The dialysis bag (Abron Exports, Haryana, India) was made ready for the experiment by soaking it in warm water for 2–5 min to make it soft enough to work efficiently. The other end was sealed with a thermo-resistant thread, and the dialysis bag was infused with PGL-SMEDDS formulation (equivalent to 7.5 mg of PGL), which was then sealed and allowed to rotate freely in 100 ml of dissolution medium kept over the stirrer. At regular intervals, one mL was withdrawn, and the aliquot of dissolution medium was substituted to keep the sink condition. An equivalent amount of PGL was suspended in a suspension and compared to the drug release from the SMEDDS formulation. PGL released was analyzed spectrophotometrically at 270 nm (Ahmad et al., 2022; Yang et al., 2019).

2.2.6.7. Determination of drug content. Pioglitazone from the SMEDDS formulation (theoretically equivalent to 7.5 mg PGL) was retrieved in 10 ml methanol. The diluted sample was centrifuged for 20 min at 5000 rpm using a tabletop centrifuge (Remi, India). The supernatant was filtered, and the pioglitazone concentration was determined using the previously reported HPLC method (Prasad et al., 2015). Briefly, the RP-HPLC system (SPI-VP, Shimadzu, Japan) with a C18 column at 25 ± 1 °C and UV-visible detector at a wavelength of 270 nm was used for analysis. The mobile phase was a 40: 60 ratio of ammonium acetate buffer: acetonitrile at a flow rate of 1.0 ml/min. The detection time for PGL was 5.85 min.

2.2.6.8. FT-IR. The FT-IR analysis of the lyophilized PGL-SMEDDS was done by the KBr disc procedure with an FT-IR spectrophotometer (Bruker, UK-MSA). Samples were dispersed with KBr and converted into translucent pellets by compressing them at a mechanical pressure of 200 psi before being scanned in a range of $4000\text{---}400\text{ cm}^{-1}$ (Padhi et al., 2016).

2.2.6.9. Analysis of thermal behavior. Pure drug and SMEDDS differential scanning calorimetry (DSC) was conducted on a Perkin Elmer Pyres 6 DSC, USA. Approximately 3 mg of each pure drug and solid SMEDDS were taken in aluminum pans and then sealed with a DSC loading puncher. An empty, crimped aluminum pan was used on the other side as a control. Under a nitrogen atmosphere, the samples were scanned at 40 to 300 °C with increments of 5 °C/min (The gaseous nitrogen was supplied at a rate of 20 ml/min and a pressure of 2 bars). The DSC peaks were noted (Khuroo et al., 2018).

2.2.6.10. Stability study of PGL-SMEDDS. For three months, PGL-SMEDDS was stored at room temperature (RT) and under accelerated conditions (40 ± 2 °C and 75 ± 5 % RH) as part of a stability study performed in accordance with ICH recommendations to assess the impact of temperature and humidity on the PGL-SMEDDS. Parameters such as Physical appearance, emulsification efficiency, drug quantity, percent transmittance, and globule size

were assessed to verify the stability of the prepared formulation during the storage period.

2.2.7. Pharmacokinetics studies

2.2.7.1. Animal husbandry. Sixteen male Wister Rats (weighing 200–250 gm) were used to conduct the pharmacokinetic study. The study was conducted in strict accordance with the guidelines established by the Institutional Animal Ethics Committee (IAEC) of Jamia Hamdard in New Delhi, India (IAEC-70-JH-1674/CPCSEA, 2021). Rats were housed in a controlled environment (23 ± 2 °C; 12 hr light /dark cycle). The rats were equally allocated into four groups each having four animals ($n = 4$) and named as control, pure drug-treated (group II), marketed tablets treated (group III), and liquid SMEDDS treated (group IV).

2.2.7.2. A bioanalytical HPLC method. Pioglitazone levels in rat plasma were determined using the RP-HPLC method. Components were separated using a LiChrospher R C18 column (5 μ m pore size; Merck, Germany) and a 60:40 combination of acetonitrile and ammonium acetate buffer as a mobile phase at flow rate of 0.8 ml/min and 25 ± 1 °C temperature. The retention time was 3.65 min and the eluent was censored at 270 nm using a PDA detector. Limits of quantitation (LOQ) and detection (LOD) were calculated to be 134.24 and 72.13 ng/ml, respectively.

2.2.7.3. Experimental protocol. Prior to the experiments, the rats had unrestricted access to water and a rat-appropriate meal (Lipton feed, Mumbai, India). Rats were made to fast overnight before being given their doses. The PGL suspension and PGL marketed tablet were prepared by suspending the required amount of PGL in 0.5% methylcellulose (MW 14000 Da, viscosity 15 cP). PGL suspension, PGL marketed tablet, and PGL-SMEDDS were administered orally using oral gavage at a dose equivalent to 3 mg/kg of PGL to Group II, Group III, and Group IV, respectively. Rats were given an i.p. injection of ketamine/xylazine (75/8 mg/kg), and then 0.5 ml of blood was taken from their tail veins at 0 (pre-dose), 1, 2, 4, 6, 8, and 24 hr, and preserved in EDTA-coated microcentrifuge tubes. After 10 min of 10,000 rpm centrifugation, the plasma was transferred and kept in a -20 °C freezer until analysis. Then plasma samples were treated with 400 μ l of ethyl acetate to deproteinize the proteins, vortexed for 2 min to prevent elution interference in the analysis, and then centrifuged at 5,000 rpm for 15 min. Evaporation of ethyl acetate was carried out in new vials, and the mobile phase was added to reconstitute the dried samples, which were then filtered and injected into the HPLC column at 20 μ l. The extravascular compartmental approach was used to derive the pharmacokinetic parameters, and the PK-Solver (Version 2.0) was used to estimate the parameters in MS-Excel-2019. (Chaudhary et al., 2019).

2.2.8. Statistics

The data are existing as the mean \pm SD of three separate replicates. One-way ANOVA was used to determine the significant level ($P < 0.05$ value is used to show statistical significance).

3. Results

3.1. Screening of excipients

Screening of SMEDDS components was done as the solubility capacity of a vehicle was critical for SMEDDS stability. The results for PGL solubility in different excipients are presented in (Fig. 1). PGL showed the highest solubility in ethyl oleate (17.72 mg/ml), followed by fish oil (14.1 mg/ml) among oils. Fish oil was mixed with ethyl oleate in a 3:1 ratio as an oil phase. The surfactant

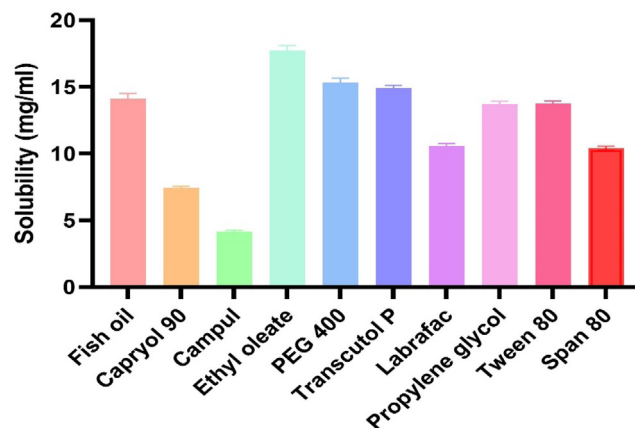


Fig. 1. Solubility of pioglitazone in various vehicles. Each value represents the mean \pm S.D. ($n = 3$).

was chosen for its PGL-solubility and its capacity to emulsify the oil phase i.e. fish oil & ethyl oleate. Among various surfactants screened for solubility, PGL showed the highest solubility in Tween[®] 80 (13.71 mg/ml). In addition, Tween[®] 80 showed good miscibility with the oil phase. Supplementary Table S1 shows the percent transmittance values and the number of inversions needed for the uniform emulsion of different dispersions. Hence, Tween[®] 80 was decided upon as the surfactant of choice. Miscibility tests were performed using the oils and a surfactant to determine the best co-surfactant to use. Transcutol HP showed good miscibility with the oils and surfactant system, so selected as a co-surfactant.

3.2. Pseudo-ternary phase diagrams construction

Determining the excipient ratio for SMEDDS is the crucial step in formulating to achieve balance during loading and prevent precipitation when diluted in GIT fluids. Thus, a phase diagram study was conducted to establish the relationship between the SMEDDS components.

Fish oil and ethyl oleate at a 3:1 ratio, Tween[®] 80, Transcutol HP, and bi-distilled water (aqueous phase) were used to construct pseudo-ternary phase diagrams. The water titration procedure was used for each combination of oil and S_{mix} individually. A water concentration of 5% to 90% of the total volume was achieved by adding the aqueous phase in 5% increments. Because the o/w interfacial tension needed to generate stable SMEDDS cannot be reduced by using a Km value of 1:1, a small microemulsion area has been accomplished. The highest microemulsion region was attained at a Km value of 4:1 when the Tween[®] 80 to Transcutol HP ratio was raised from 1:1 to 4:1 (Supplementary Figure S1). Small globules were formed when there was a high Tween[®] 80 concentration because it reduces interfacial tension and enables surfactants to diffuse into the aqueous phase. Besides, interfacial tension was further reduced by the Transcutol HP, which makes a flexible film, increases the system's entropy, and changes the polarity, density, refractive index, and viscosity of the aqueous phase. So, the Km value of 4:1 was therefore selected for further exploration.

3.3. Optimization of concentration of oil and S_{mix}

Five center, four axial, and four factorial runs with varying oil and S_{mix} concentrations were automatically created using the CCD design. As per the proposed runs, the formulations were prepared and the particle size, % transmittance, and PDI were noted (Table 2). These observations were recorded to study the influence

Table 2

CCD-observed PGL-SMEDDS runs along with actual dependent variables values and the regression analyses of specified responses.

Run	Space type	Oil (mg) (X1)	S _{mix} (mg) (X2)	Particle size (nm)(Y1)	% Transmittance (Y2)	PDI (Y3)	
1	Center	16	80	144.5	98.12	0.193	
2	Center	16	80	146.3	98.2	0.218	
3	Axial	0.443651	80	190	98.5	0.099	
4	Factorial	5	65	152	96.4	0.138	
5	Axial	31.5563	80	295	89	0.265	
6	Axial	16	58.7868	160	93.7	0.205	
7	Center	16	80	148.3	98	0.226	
8	Center	16	80	140.2	98.9	0.244	
9	Factorial	27	65	251.2	89	0.275	
10	Factorial	5	95	150	98.1	0.111	
11	Factorial	27	95	210	91.3	0.218	
12	Center	16	80	146.5	98.2	0.208	
13	Axial	16	101.213	120	97.3	0.174	
Optimized PGL-SMEDDS	16	80	142	98.1	0.232		
Quadratic model	R2	Adjusted R2	Predicted R2	Adeq. Precision	SD	Mean	C.V. %
Y1	0.9975	0.9958	0.9894	78.4487	3.27	173.38	1.89
Y2	0.9851	0.9745	0.9112	25.4622	0.5897	95.75	0.6159
Y3	0.9532	0.9198	0.8940	16.3285	0.0155	0.1980	2.82

of independent factors i.e. oil and S_{mix} on the dependent variables i.e. particle size, % transmittance, and PDI.

The results of the tested dependent variables, particle size (Y1), % T (Y2), and PDI (Y3), fall within the ranges of 120–295 nm, 89–98.9%, and 0.099–0.275, respectively. A quadratic model provided the greatest fit for the data from all three responses, suggesting that the model was statistically significant (Supplementary Table S2,3,4). “Predicted R2” values were consistent with “Adjusted R2” values for all responses (i.e. the difference < 0.2) (Table 2). Adeq. Precision is more than 4 for the three responses which indicates the ratio of the signal to the noise.

Equation (1) shows that oil concentration and S_{mix} were major factors in determining droplet size. The 3D response surface plots (Fig. 2A) showed that the droplet size raised with the oil concentration and decreased with the S_{mix} concentration. The formulation is stabilized by the high concentration of surfactant by forming a barrier on the SMEDDS' surface, inhibiting them from aggregating into bigger particles.

$$Y1 = 145.16 + 38.4616 \times A + -12.4711 \times B + -9.8 \times AB + 48.5575 \times A^2 + -2.6925 \times B^2 \dots \dots Eq \quad (1)$$

Polynomial Equation (2) showed how oil and surfactant concentration affected the percent of transmittance. The transmittance study showed an inverse relationship with oil concentration and a positive relationship with S_{mix} concentration (Fig. 2B). When the percentage of transmittance was high, it showed that the particles were evenly dispersed, whereas a low number indicated a turbid formulation (Solanki et al., 2022).

$$Y2 = 98.284 + -3.45438 \times A + 1.1364 \times B + 0.15 \times AB + -2.49825 \times A^2 + -1.62325 \times B^2 \quad (2)$$

Particle size distribution in a formulation is represented by the PDI. As the surfactant concentrations increase, polydispersity falls as the drug is completely coated, and as the concentration decreases, the droplet size increases. Polynomial Equation (3) depicting the effect of oil and surfactant concentrations on polydispersity.

$$Y3 = 0.2178 + 0.0598449 \times A + -0.0159801 \times B + -0.0075 \times AB + -0.0179625 \times A^2 + -0.0142125 \times B^2 \quad (3)$$

Response prediction is possible for a range of factor levels using the equation stated in terms of coded factors. Fig. 2C showed that the PDI of the SMEDDS was significantly influenced by oil concentration, with the PDI growing linearly with increasing oil levels. S_{mix} had a nonsignificant impact on the PDI.

3.3.1. Validation of the CCD

The optimal PGL-SMEDDS formulation contents are the primary focus of the CCD-based systematic optimization. To maximize SMEDDS absorption and stability, the optimal polynomial model was utilized to guide a numerical optimization procedure with desired values for all response variables, such as “minimum” particle size, “minimum” PDI, and maximum % transmittance. The optimal PGL-SMEDDS formulation was predicted by the design expert CCD software by means of quadratic modeling for all dependent variables and constraints tailored to them. According to CCD, the final report for optimized PGL-SMEDDS was comprised of 16 mg oil (Fish oil: Ethyl oleate, 3:1) and 80 mg S_{mix} (Tween® 80: Transcutol HP, 4:1). Graphical optimization was utilized to produce an overlay plot (Fig. 2D), which shows the predicted values of all dependent variables for the optimal PGL-SMEDDS combination. This optimized PGL-SMEDDS has anticipated values of 145.16 nm, 98.2% transmittance, and PDI of 0.217 (Fig. 2D). Whereas, 142.0 nm, 98.1%, and 0.232 were measured as the actual responses after applying this combination (Table 2). Considering that the prediction error between the model and the observed data was <5%, we concluded that the model was adequate and reliable (Alhalmi et al., 2022a).

3.4. Characterization of PGL-SMEDDS

3.4.1. Viscosity and %Transmittance

To ensure that SMEDDS is physically stable, the viscosity character is evaluated. Also, SMEDDS dispersion in an aqueous medium is critical since the low emulsification rate of more viscous formulations can affect drug release and bioavailability (Patel and Sawant, 2019). The viscosity was 59.6 ± 2.4cP, low enough to facilitate quick emulsification. The % transmittance value was 98 ± 1.30 %, indicating the clarity by visual check, which is a fundamental requirement for microemulsion.

3.4.2. Robustness to dispersion

Distilled water, pH 1.2, and pH 7.4 were used to dilute PGL-SMEDDS. No precipitation nor phase separation occurred in any

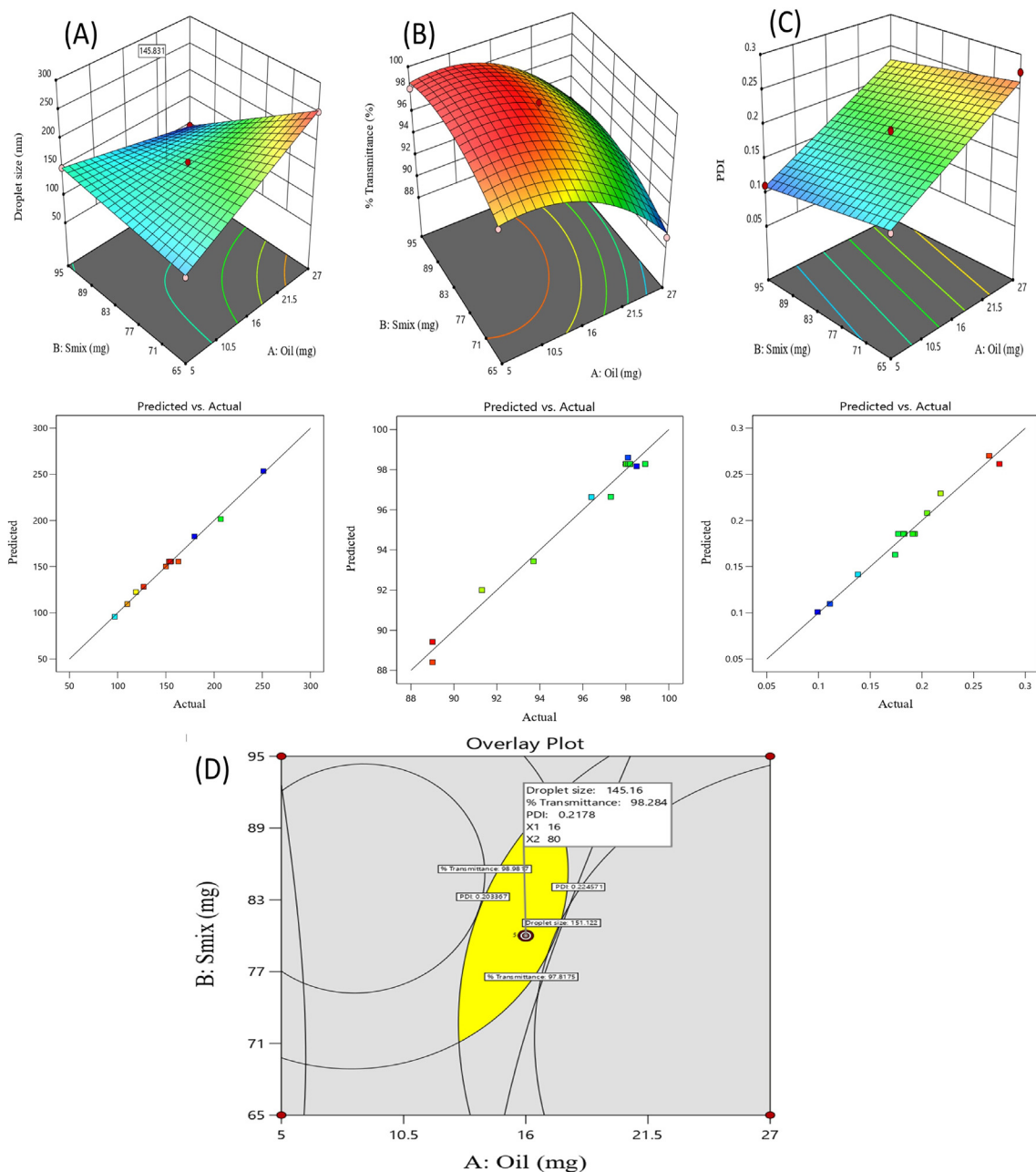


Fig. 2. Response surface curve: Effect of oil and S_{mix} on particle size (A), %transmittance (B), and PDI (C) and Overlay plot (D): The yellow region denotes the design space and the optimal PGL-SMEDDS displayed by the flag mark.

of the test media or dilutions. According to this, aqueous phase pH does not affect microemulsion formulation.

3.4.3. Self-emulsification time test

Emulsification time is a significant parameter for determining the spontaneity of microemulsion development, so SMEDDS should be dispersed immediately in the GIT fluid following oral administration. The PGL-SMEDDS emulsification time was 40.0 ± 2.0 sec, indicating that the system will effectively self-micro emulsify and be ready to disperse in GIT fluid. This may be due to Transcutol HP, which significantly affects interfacial characteristics such as spontaneous arrangement, polarity, thickness, and interfacial tension (Patel and Sawant, 2019).

3.4.4. Globule size, PDI, zeta potential and TEM

The mean globule size of the developed PGL-SMEDDS was 142 nm with a PDI of 0.232 (Fig. 3A). Zeta potential was measured at -20.9 mV (Fig. 3B), which, in combination with the adsorbed surfactant layer, provides the repulsion required to prevent globular coalescence. This result confirms the PGL-SMEDDS physical stability. TEM was also used to observe the shape of the microemulsion generated from the SMEDDS formulation. (Fig. 3C) illustrates the spherical shape of the emulsion droplets in the absence of aggregation.

3.4.5. Drug content

The drug content of the PGL-SMEDDS was determined using the HPLC method, with 7.5 mg of pioglitazone assumed to be 100%. The PGL content of the PGL-SMEDDS was found to be 98.61%, which is

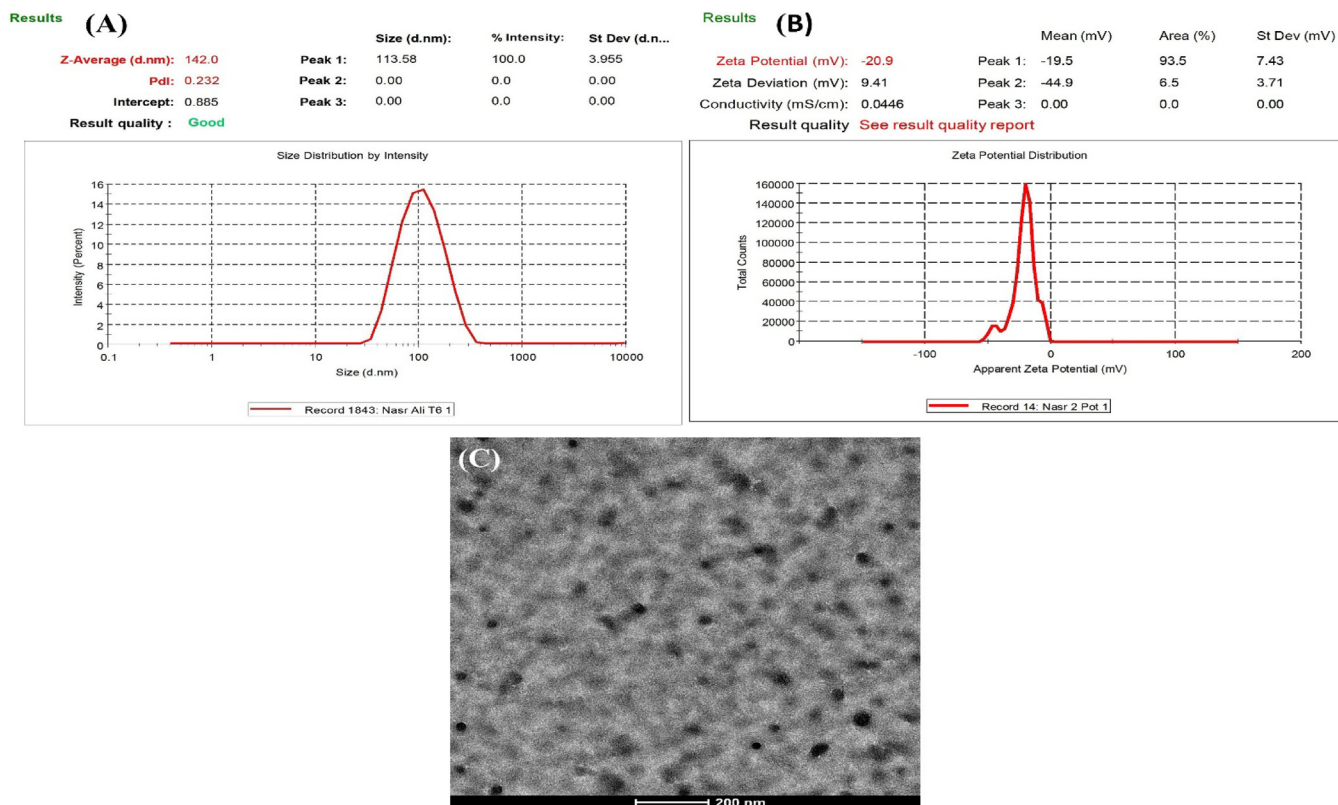


Fig. 3. Morphology of the optimized PGL-SMEDDS: Globule size (A), Zeta potential (B), and TEM (C).

within the specified range (90–110%) defined in IP 2010 and confirms the PGL-SMEDDS stability.

3.4.6. FT-IR analysis

FTIR analysis has been conducted to detect any potential interactions between the SMEDDS components and the drug. Absorption peaks at 3337.04, 2829.82, 1739.66, and 1682.88 cm^{-1} in the FTIR spectrum of PGL-SMEDDS correspond to the N–H stretching vibration, C–H aliphatic stretching, and two carbonyl functions, respectively (Fig. 4A2). Slight variations in the drug's characteristic peaks have been seen in PGL-SMEDDS in comparison to the pure PGL FTIR spectrum (Fig. 4A1), which can be ascribed to non-binding drug interactions with SMEDDS components (Kanwal et al., 2019). FTIR evaluation confirms the good chemical stability of PGL inside the optimized PGL-SMEDDS formulation.

3.4.7. Differential scanning calorimetry

The thermotropic characteristics and thermal character of the drug and excipients utilized in PGL-SMEDDS formulations were determined using DSC. An exothermic peak temperature of 196.63 °C was reported as the melting point of PGL (Fig. 4B1). The DSC thermogram of the lyophilized PGL-SMEDDS (Fig. 4B2) shows an exothermic peak at 126.947 °C, which is related to the melting point of the carrier, microcrystalline cellulose (de Oliveira et al., 2017). The absence of the crystalline peak of PGL in the lyophilized PGL-SMEDDS suggested uniform drug adsorption on the carrier. It was probably due to the molecular dispersion/dissolution of PGL in the SMEDDS components or interactions at the molecular level.

3.4.8. Drug released study in-vitro

Since a drug is released as a free molecule, micelle, or microemulsion droplet upon contact with water, traditional in-

vitro dissolution methods are not ideal for studying the in-vitro dissolution of SMEDDS. So particular drug molecules should be segregated from micelles or microemulsions (Javed Ahmad, Kanchan Kohli, 2011). Dissolution studies using a dialysis bag ensure consistent medication release. Since the PGL release from SMEDDS was shown to be constant regardless of the pH of the dissolving medium (pH 1.2 and pH 6.8), it may be concluded that the PGL release from SMEDDS is pH-independent (Fig. 5A&B). A higher drug release (59.13%) was observed in the first two hr at pH 1.2 than at pH 6.8 (31.34%) (Supplementary Table S5, S6). Most of the PGL was dissolved in the oil phase, with a reasonable proportion dispersed on the interface of the oil and water, which may lead to rapid release into the water when SMEDDS formulations were put into aqueous media with gentle agitation. Otherwise, diffusion through the droplet surface may limit pioglitazone's release in the oil phase. The release profile of the PGL from SMEDDS was 15 and 1.6 times more than that of the suspension in both PBS (pH 6.8) (Fig. 5B) and 0.1 N HCl (pH 1.2) (Fig. 5A), respectively.

Many mathematical models namely, Zero order, First order, Korsmeyer-peppas, and Higuchi models were used to fit the pioglitazone dissolution curves from SMEDDS formulations in order to investigate the release mechanism. Results show that the first-order model is the best way to study how PGL is released from SMEDDS formulation at both pHs because the highest correlation coefficient (R^2) value was obtained (Supplementary Figure S2, S3).

3.4.9. Stability study

The results for the stability parameters measured are given in Table 3. The SMEDDS formulation was analyzed for self-emulsification time, assay for drug content, % transmittance, and globule size. SMEDDS remained clear at all storage conditions, i.e., no drug precipitation or cloudiness marks. In other words, the medication maintained its solubilized state both at ambient

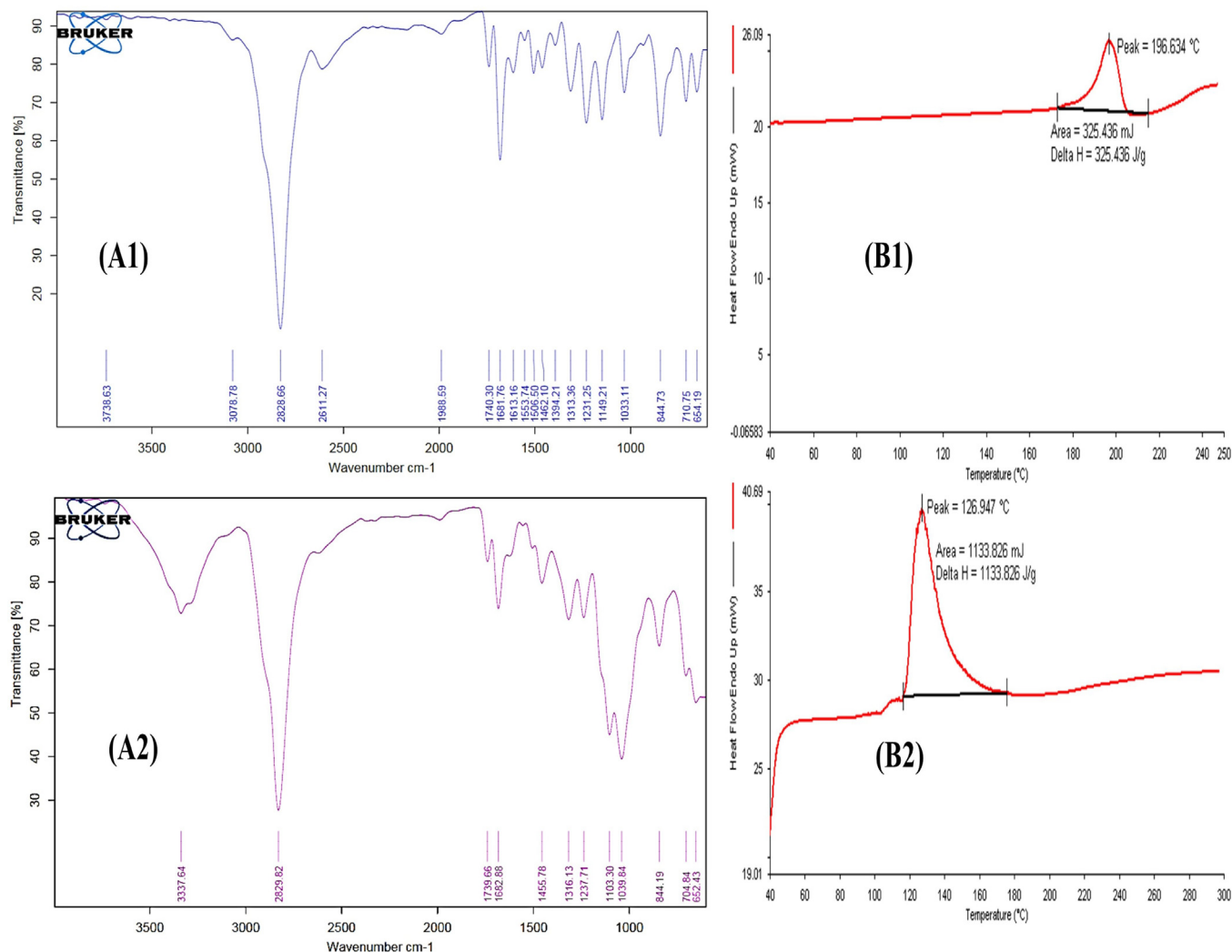


Fig. 4. (A1) FT-IR spectra of Pure PGL, (A2) FT-IR spectra of PGL-loaded SMEDDS, (B1) DSC of Pure PGL and (B2) DSC of PGL-loaded SMEDDS.

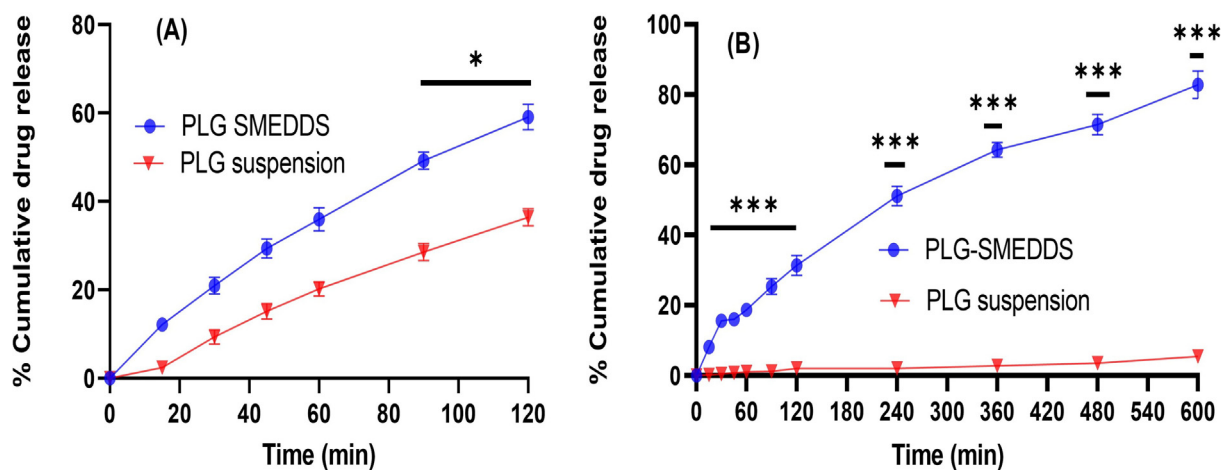


Fig. 5. Drug released from PLG-SMEDDS and PLG suspension in (A) 0.1 N HCl, and (B) PBS (pH 6.8). Each value represents the mean \pm S.D. (n = 3). * and *** represent $p < 0.05$ and $p < 0.001$ respectively, compared with PGL suspension.

temperature and accelerated conditions (40 ± 2 °C/ 75 ± 5 %RH). Similarly, self-emulsification time, % transmittance, and global size show insignificant changes, and the microemulsion system was

considered stable upon dilution with uniform globule size distribution. In addition, after 3 months of storage, there was no discernible drop in PGL content for SMEDDS, demonstrating the

Table 3
Stability parameters were measured during three months for the prepared PGL-SMEDDS.

Condition	Parameters/ Time(days)	0	30	60	90
At room temperature	Visual inspection	clear	clear	clear	clear
	Self-emuls. time (sec)	40.0 ± 2.0	41.0 ± 2.0	41.0 ± 2.0	42 ± 2.0
	Drug content	98.61 ± 0.17	98.26 ± 0.17	98.15 ± 0.28	98.10 ± 0.23
	%Transmittance	98.13 ± 0.47	98.33 ± 0.47	97.41 ± 0.45	97.20 ± 0.64
	Globule size (nm)	142	142.3	142.5	143
Accelerated stability conditions (40 °C ± 2 °C/75 ± 5 %RH)	Visual inspection	clear	clear	clear	clear
	Self-emuls. time (sec)	40.0 ± 2.0	42.0 ± 2.0	43.0 ± 2.0	43.0 ± 2.0
	Drug content	98.61 ± 0.17	98.14 ± 0.17	98.11 ± 0.38	98.04 ± 0.86
	%Transmittance	98.13 ± 0.47	98.12 ± 0.47	97.20 ± 0.34	97.06 ± 0.14
	Globule size(nm)	142	142.8	143	143.4

drug's continued chemical stability. As a result, the PGL-SMEDDS was found to be stable at both room temperature and in accelerated conditions (40 °C ± 2 °C/75 ± 5 %RH).

3.4.10. Pharmacokinetics studies

In albino Wistar rats, the plasma concentration–time profile and pharmacokinetic data for PGL suspension, PGL-marketed tablet, and PGL-SMEDDS are displayed in Fig. 6 and Table 4, respectively. As a result of the rapid self-micro emulsification of the drug in the GI lumen, the PGL-SMEDDS showed high plasma levels in rats. The C_{max} and AUC values showed a statistically significant increase in PGL absorption ($p < 0.05$). The AUC_{0-t} of PGL-SMEDDS after oral administration was 3.4 and 1.4 times more than that of PGL suspension and PGL-marketed tablets, respectively. The sustained release of PGL from both the PGL-SMEDDS and commercially available tablets could explain why these formulations have a longer time to achieve maximum plasma concentration (T_{max}) than PGL suspension. Maintaining a constant plasma drug level using SMEDDS supported the increased $t_{1/2}$ value.

4. Discussion

Drugs must be dissolved for SMEDDS because studies have shown that a steeper concentration gradient propels the medication through the gastrointestinal tract, increasing its bioavailability. Fish oil includes multi-component fatty acids, which lead to poor dispersity and low water solubility, limiting its usefulness as a standalone oil phase in SMEDDS. Therefore, fish oil was mixed with ethyl oleate in a 3:1 ratio to attain the goal of our study, which is to incorporate a high amount of fish oil into the oil phase.

The prepared SMEDDS showed satisfactory levels for droplet size, PDI, and zeta potential. Smaller droplets provide more surface area for drug absorption and a faster release rate, making droplet size an important parameter in evaluating SMEDDS (Choi et al., 2014). Particle dispersion uniformity is quantified by the PDI, and dispersion stability is quantified by the zeta potential. PGL release was not impacted by the pH medium by using SMEDDS, and the release of PGL from the suspension was pH-dependent (Fig. 5). As a result, the barrier of poor dissolving in GIT may have been overcome, leading to improved absorption of pioglitazone from SMEDDS. The higher release from the drug suspension in 0.1 N HCl (36.4%) than in PBS (pH 6.8) (5.46%) is due to the PGL used in this research was in a salt form (pioglitazone HCl), which has more ionization in an acidic medium. The enhanced C_{max} and AUC values could be the effect of the enhanced SMEDDS formulation increasing the solubility and/or dissolving rate of PGL. Additionally, excipients such as Tween® 80 and Transcutol HP included in the SMEDDS formulation have been reported to inhibit P-gp and CYP₄₅₀ (Al-Kandari et al., 2020; Markiewicz et al., 2019) and thus promote intestinal absorption of PGL. The pharmacokinetic profile confirms the in vitro release results showing that pioglitazone of the suspension was primarily absorbed from the stomach which can be interpreted by the higher solubility of PGL in an acidic pH and the absence of overexpression of P-gp in the stomach. However, SMEDDS showed a sustained release of pioglitazone throughout the GI tract. Besides, small intestine absorption of the PGL was also found to be unimpeded. Future works should focus on the synergistic effect of fish oil-based PGL-SMEDDS on insulin resistance. Such data would provide useful insights into

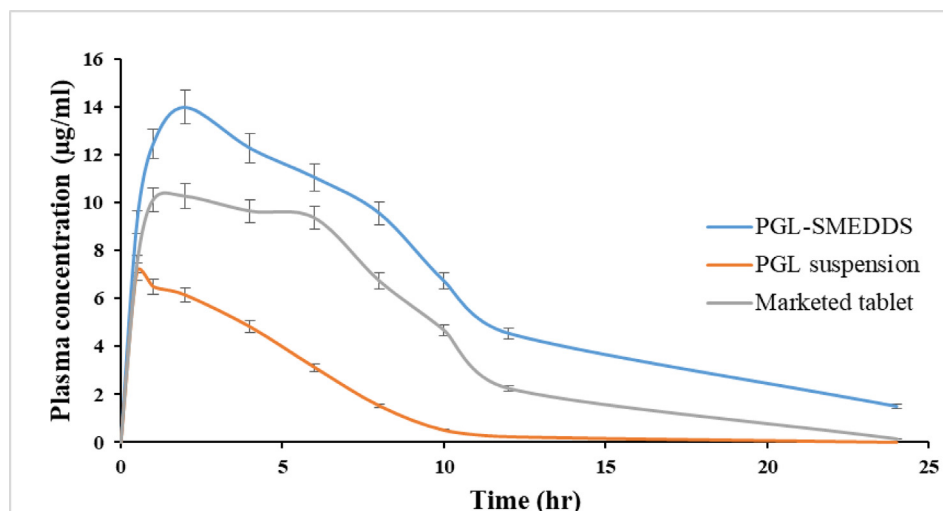


Fig. 6. Plasma concentration–time profile of PGL-SMEDDS, Marketed tablet, and PGL suspension. Each value represents the mean ± S.D. (n = 3).

Table 4

PGL-SMEDDS compared to PGL-marketed tablets and PGL suspension in terms of pharmacokinetic characteristics in rats (3 mg/kg).

PK parameters	Unit	PGL-susp.	Marketed tablets	PGL-SMEDDS
$t_{1/2}$	h	1.5 ± 0.5	2.9 ± 0.3	4.1 ± 0.2
T_{max}	h	0.5 ± 0.4	2 ± 0.25	2 ± 0.3
C_{max}	µg/ml	7.13 ± 0.341	10.27 ± 0.197	13.98 ± 0.315 ^a
AUC_{0-t}	µg/ml ^{*h}	44.28 ± 0.274	108.93 ± 0.445	151.54 ± 0.386 ^a
$AUC_{0-inf,obs}$	µg/ml ^{*h}	44.81 ± 0.334	109.54 ± 0.299	164.93 ± 0.344 ^a
$AUMC_{0-inf,obs}$	µg/ml ^{*h} ²	155.46 ± 0.497	675.01 ± 0.562	1600.46 ± 0.982 ^a

Notes: Each value represents the mean ± S.D. (n = 3). ^a P < 0.05 compared with PGL suspension.

Abbreviations: C_{max} , maximum drug concentration; T_{max} , time taken to reach maximum drug concentration;

$t_{1/2}$, time required for a quantity to reduce to half its initial value; AUC, area under the curve; PGL-suspension, pioglitazone suspension; PGL-SMEDDS, pioglitazone loaded self-microemulsifying drug delivery system.

how fish oil-based PGL-SMEDDS behaves and the real limits of its activity against insulin resistance.

5. Conclusions

This is the first study that successfully developed a Self-Microemulsifying Drug Delivery System (SMEDDS) using fish oil to enhance the oral delivery of pioglitazone (PGL). The formulated SMEDDS exhibited optimal dosage form properties, including appropriate globule size, globule distribution, morphology, thermodynamic stability, and self-emulsification time, both in vitro and in vivo. The in vitro release study demonstrated first-order kinetics, while the in vivo study revealed significantly higher AUC_{0-t} values for PGL-SMEDDS compared to PGL suspension and PGL-marketed tablets, with 3.4-fold and 1.4-fold increases, respectively. Furthermore, the developed SMEDDS demonstrated sustained release of pioglitazone throughout the gastrointestinal tract without compromising drug absorption in the small intestine. Importantly, the dissolution of PGL-SMEDDS was independent of pH media, overcoming the challenge of poor PGL solubility in higher pH environments. These findings highlight the potential of fish oil-based PGL-SMEDDS as an advanced option for improving the oral bioavailability of pioglitazone while harnessing the synergistic effects of fish oil in improving insulin resistance and reducing potential side effects associated with PGL. Future studies investigating the synergistic pharmacological effects of fish oil-based PGL-SMEDDS on rats are highly recommended.

Declaration of Competing Interest

The authors declare that they have no known competing financial interests or personal relationships that could have appeared to influence the work reported in this paper.

Funding

Princess Nourah bint Abdulrahman University Researchers Supporting Project number (PNURSP2023R141), Princess Nourah bint Abdulrahman University, Riyadh, Saudi Arabia. Thankful also to Researchers Supporting Project number (RSPD2023R732), King Saud University, Riyadh, Saudi Arabia.

Acknowledgments

The authors extend their appreciation to Princess Nourah bint Abdulrahman University Researchers Supporting Project number (PNURSP2023R141), Princess Nourah bint Abdulrahman University, Riyadh, Saudi Arabia. Thankful also to Researchers Supporting Project number (RSPD2023R732), King Saud University, Riyadh, Saudi Arabia.

Appendix A. Supplementary material

Supplementary data to this article can be found online at <https://doi.org/10.1016/j.sjbs.2023.103778>.

References

- Adil, M., Khan, R.A., Ghosh, P., Venkata, S.K., Kandhare, A.D., Sharma, M., 2018. Pioglitazone and risk of bladder cancer in type 2 diabetes mellitus patients: A systematic literature review and meta-analysis of observational studies using real-world data. *Clin. Epidemiol. Glob. Heal.* 6, 61–68. <https://doi.org/10.1016/j.cegh.2017.08.002>.
- Javed Ahmad, Kanchan Kohli, S.R.M. & S.A., 2011. Formulation of Self-Nanoemulsifying Drug Delivery System for Telmisartan with Improved Dissolution and Oral Bioavailability Formulation of Self-Nanoemulsifying Drug Delivery System for Telmisartan with Improved Dissolution and Oral Bioavailability. *J. Dispers. Sci. Technol.* 32, 958–968. Doi: 10.1080/01932691.2010.488511.
- Ahmad, S., Khan, I., Pandit, J., Emad, N.A., Bano, S., Dar, K.I., Rizvi, M.M.A., Ansari, M. D., Aqil, M., Sultana, Y., 2022. Brain targeted delivery of curmestine using chitosan coated nanoparticles via nasal route for glioblastoma treatment. *Int. J. Biol. Macromol.* 221, 435–445. <https://doi.org/10.1016/j.ijbiomac.2022.08.210>.
- Alhalmi, A., Amin, S., Beg, S., Al-Salahi, R., Mir, S.R., Kohli, K., 2022a. Formulation and optimization of naringin loaded nanostructured lipid carriers using Box-Behnken based design: In vitro and ex vivo evaluation. *J. Drug Deliv. Sci. Technol.* 74. <https://doi.org/10.1016/j.jddst.2022.103590> 103590.
- Alhalmi, A., Amin, S., Khan, Z., Beg, S., Al kamaly, O., Saleh, A., Kohli, K., 2022b. Nanostructured Lipid Carrier-Based Codelivery of Raloxifene and Naringin: Formulation, Optimization, In Vitro, Ex Vivo, In Vivo Assessment, and Acute Toxicity Studies. *Pharmaceutics* 14, 1–27. Doi: 10.3390/pharmaceutics14091771.
- Al-Kandari, B.M., Al-Soraj, M.H., Hedaya, M.A., 2020. Dual formulation and interaction strategies to enhance the oral bioavailability of paclitaxel. *J. Pharm. Sci.* 109, 3386–3393. <https://doi.org/10.1016/j.xphs.2020.07.027>.
- Amery, C.M., Round, R.A., Smith, J.M., Nattrass, M., 2000. Elevation of plasma fatty acids by ten-hour intralipid infusion has no effect on basal or glucose-stimulated insulin secretion in normal man. *Metabolism* 49, 450–454. [https://doi.org/10.1016/S0026-0495\(00\)80007-4](https://doi.org/10.1016/S0026-0495(00)80007-4).
- Azoulay, L., Yin, H., Filion, K.B., Assayag, J., Majdan, A., Pollak, M.N., Suissa, S., 2012. The use of pioglitazone and the risk of bladder cancer in people with type 2 diabetes: Nested case-control study. *BMJ* 344, 1–11. <https://doi.org/10.1136/bmj.e3645>.
- Boden, G., 1996. Fatty acids and insulin resistance. *Diabetes Care* 19, 394–395. <https://doi.org/10.2337/diacare.19.4.394>.
- Bolko, K., Zvonar, A., Gas, M., 2013. Mixed lipid phase SMEDDS as an innovative approach to enhance resveratrol solubility. *Drug Dev. Ind. Pharm.* 40 (1), 102–109. <https://doi.org/10.3109/03639045.2012.749888>.
- Chaudhary, S., Aqil, M., Sultana, Y., Kalam, M.A., 2019. Self-nanoemulsifying drug delivery system of nabumetone improved its oral bioavailability and anti-inflammatory effects in rat model. *J. Drug Deliv. Sci. Technol.* 51, 736–745. <https://doi.org/10.1016/j.jddst.2018.04.009>.
- Choi, H., Yong, C.S., Kim, J.O., 2014. Application of Box-Behnken design in the preparation and optimization of fenofibrate-loaded self-microemulsifying drug delivery system (SMEDDS). *J. Microencapsul.* 31, 31–40. <https://doi.org/10.3109/02652048.2013.805837>.
- de Oliveira, G.G., Feitosa, A., Loureiro, K., Fernandes, A.R., Souto, E.B., Severino, P., 2017. Compatibility study of paracetamol, chlorpheniramine maleate and phenylephrine hydrochloride in physical mixtures. *Saudi Pharm. J.* 25, 99–103. <https://doi.org/10.1016/j.sjps.2016.05.001>.
- Eissa, L.A., Abdel-Rahman, N., Eraky, S.M., 2015. Effects of omega-3 fatty acids and pioglitazone combination on insulin resistance through fibroblast growth factor 21 in type 2 diabetes mellitus. *Egypt. J. Basic Appl. Sci.* 2, 75–86. <https://doi.org/10.1016/j.ejbas.2015.01.002>.

- Elbary, A.A., Kassem, M.A., Abou Samra, M.M., Khalil, R.M., 2008. Formulation and hypoglycemic activity of pioglitazone-cyclodextrin inclusion complexes. *Drug Discov. Ther.* 2, 94–107.
- Emad, N.A., Ahmed, B., Alhalmi, A., Alzobaidi, N., Al-Kubati, S.S., 2021. Recent progress in nanocarriers for direct nose to brain drug delivery. *J. Drug Deliv. Sci. Technol.* 64. <https://doi.org/10.1016/j.jddst.2021.102642>
- Gao, H., Geng, T., Huang, T., Zhao, Q., 2017. Fish oil supplementation and insulin sensitivity : a systematic review and meta- analysis. *Lipids Heal. Dis.* 16. <https://doi.org/10.1186/s12944-017-0528-0>.
- Hasan, M.M., El-Shal, A.S., Mackawy, A.M.H., Ibrahim, E.M., Abdelghany, E.M.M.A., Saeed, A.A., El-Gendy, J., 2020. Ameliorative effect of combined low dose of Pioglitazone and omega-3 on spermatogenesis and steroidogenesis in diabetic rats. *J. Cell. Biochem.* 121, 1524–1540. <https://doi.org/10.1002/jcb.29388>.
- Huo, T., Tao, C., Zhang, M., Liu, Q., Lin, B., Liu, Z., 2018. Preparation and comparison of tacrolimus-loaded solid dispersion and self- microemulsifying drug delivery system by in vitro / in vivo evaluation. *Eur. J. Pharm. Sci.* 114, 74–83. <https://doi.org/10.1016/j.ejps.2017.12.002>.
- Iizuka, Y., Kim, H., Izawa, T., Sakurai, K., Hirako, S., Wada, M., Matsumoto, A., 2016a. Protective effects of fish oil and pioglitazone on pancreatic tissue in obese KK mice with type 2 diabetes. *Prostaglandins Leukot. Essent. Fat. Acids* 115, 53–59. <https://doi.org/10.1016/j.plefa.2016.10.007>.
- Iizuka, Y., Kim, H., Nakasatomi, M., Izawa, T., Hirako, S., Matsumoto, A., 2016b. Fish oil prevents excessive accumulation of subcutaneous fat caused by an adverse effect of pioglitazone treatment and positively changes adipocytes in KK mice. *Toxicol. Reports* 3, 4–14. <https://doi.org/10.1016/j.toxrep.2015.11.003>.
- Iizuka, Y., Kim, H., Hirako, S., Chiba, K., 2018. Benefits of combination low-dose pioglitazone plus fish oil on aged type 2 diabetes mice. *J. Food Drug Anal.* 26, 1265–1274. <https://doi.org/10.1016/j.jfda.2018.05.008>.
- Jump, D.B., 2008. N-3 polyunsaturated fatty acid regulation of hepatic gene transcription. *Curr. Opin. Lipidol.* 19, 242–247. <https://doi.org/10.1097/MOL.0b013e32822ffa6a.N-3>.
- Kalin, M.F., Goncalves, M., John-Kalarickal, J., Fonseca, V., 2017. Pathogenesis of type 2 diabetes mellitus. *Princ. Diabetes Mellit.* Third Ed., 267–277 https://doi.org/10.1007/978-3-319-18741-9_13.
- Kanwal, T., Kawish, M., Maharjan, R., Ghaffar, I., Saad, H., Imran, M., Perveen, S., Saifullah, S., Usman, S., Raza, M., 2019. Design and development of permeation enhancer containing self-nanoemulsifying drug delivery system (SNEDDS) for ceftriaxone sodium improved oral pharmacokinetics. *J. Mol. Liq.* 289. <https://doi.org/10.1016/j.molliq.2019.11.1098>
- Khuroo, T., Verma, D., Khuroo, A., Ali, A., Iqbal, Z., 2018. Simultaneous delivery of paclitaxel and erlotinib from dual drug loaded PLGA nanoparticles: Formulation development, thorough optimization and in vitro release. *J. Mol. Liq.* 257, 52–68. <https://doi.org/10.1016/j.molliq.2018.02.091>.
- Liu, C.-S., Chen, L., Hu, Y.-N., Dai, J.-L., Ma, B., Tang, Q.-F., Tan, X.-M., 2020. Self-microemulsifying drug delivery system for improved oral delivery and hypnotic efficacy of ferulic acid. *Int. J. Nanomed.* 15, 2059–2070. <https://doi.org/10.2147/IJN.S240449>.
- Mamtani, R., Haynes, K., Bilker, W.B., Vaughn, D.J., Strom, B.L., Glanz, K., Lewis, J.D., 2012. Association Between Longer Therapy With Thiazolidinediones and Risk of Bladder Cancer : A Cohort Study 1411–1421. <https://doi.org/10.1093/jnci/djs328>.
- Markiewicz, A., Strömval, A.M., Björklund, K., Eriksson, E., 2019. Generation of nano- and micro-sized organic pollutant emulsions in simulated road runoff. *Environ. Int.* 133. <https://doi.org/10.1016/j.envint.2019.105140>
- Martins, A.R., Crisma, A.R., Masi, L.N., Amaral, C.L., Marzuca-Nassar, G.N., Bomfim, L. H.M., Teodoro, B.G., Queiroz, A.L., Serdan, T.D.A., Torres, R.P., Mancini-Filho, J., Rodrigues, A.C., Alba-Loureiro, T.C., Pithon-Curi, T.C., Gorjao, R., Silveira, L.R., Curi, R., Newsholme, P., Hirabara, S.M., 2018. Attenuation of obesity and insulin resistance by fish oil supplementation is associated with improved skeletal muscle mitochondrial function in mice fed a high-fat diet. *J. Nutr. Biochem.* 55, 76–88. <https://doi.org/10.1016/j.jnutbio.2017.11.012>.
- McCormick, J.J., King, K.E., Dokladny, K., Mermier, C.M., 2019. Effect of acute aerobic exercise and rapamycin treatment on autophagy in peripheral blood mononuclear cells of adults with prediabetes. *Can. J. Diabetes* 43, 457–463. <https://doi.org/10.1016/j.JCJD.2019.04.005>.
- Mohit, Kumar, P., Solanki, P., Mangla, B., Aggarwal, G., 2022. Formulation Development, Optimization by Box-Behnken Design, and In Vitro Characterization of Gefitinib Phospholipid Complex Based Nanoemulsion Drug Delivery System. *J. Pharm. Innov.* <https://doi.org/10.1007/s12247-022-09690-6>.
- Padhi, S., Mirza, M.A., Verma, D., Khuroo, T., Panda, A.K., Talegaonkar, S., Khar, R.K., Iqbal, Z., 2016. Revisiting the nanoformulation design approach for effective delivery of topotecan in its stable form: an appraisal of its in vitro behavior and tumor amelioration potential. *Drug Deliv.* 23, 2827–2837. <https://doi.org/10.3109/10717544.2015.1105323>.
- Patel, M.H., Sawant, K.K., 2019. Self microemulsifying drug delivery system of lurasidone hydrochloride for enhanced oral bioavailability by lymphatic targeting: In vitro, Caco-2 cell line and in vivo evaluation. *Eur. J. Pharm. Sci.* 105027. <https://doi.org/10.1016/j.ejps.2019.105027>.
- Permanente, K., California, N., 2011. Risk of Bladder Cancer Among Diabetic 34. <https://doi.org/10.2337/dc10-1068>.
- Prajapat, M.D., Patel, N.J., Bariya, A., Patel, S.S., Butani, S.B., 2017. Formulation and evaluation of self-emulsifying drug delivery system for nimodipine, a BCS class II drug. *J. Drug Deliv. Sci. Technol.* 39, 59–68. <https://doi.org/10.1016/j.jddst.2017.02.002>.
- Prajapat, M.D., Patel, N.J., Bariya, A., Patel, S.S., Butani, S.B., 2017. Formulation and evaluation of self-emulsifying drug delivery system for nimodipine, a BCS class II drug. *J. Drug Deliv. Sci. Technol.* 39, 59–68. <https://doi.org/10.1016/j.jddst.2017.02.002>.
- Prasad, P.S., Imam, S.S., Aqil, M., Rizwan, M., Sultana, Y., Ali, A., 2015. Validated reversed phase HPLC method for determination of pioglitazone hydrochloride in bulk drug and tablet formulations 1. *J. Anal. Chem.* 70, 744–745. <https://doi.org/10.1134/S106193481506012X>.
- Sinha, B., Ghosal, S., 2020. Assessing the need for pioglitazone in the treatment of patients with type 2 diabetes: a meta-analysis of its risks and benefits from prospective trials. *Sci. Rep.* 10, 1–9. <https://doi.org/10.1038/s41598-020-72967-8>.
- Solanki, P., Ansari, M.D., Alam, M.I., Aqil, M., Ahmad, F.J., Sultana, Y., 2022. Precision engineering designed phospholipid-tagged pamidronate complex functionalized SNEDDS for the treatment of postmenopausal osteoporosis. *Drug Deliv. Transl. Res.* Springer, US. <https://doi.org/10.1007/s13346-022-01259-7>.
- Tan, S.Y., Mei Wong, J.L., Sim, Y.J., Wong, S.S., Mohamed Elhassan, S.A., Tan, S.H., Ling Lim, G.P., Rong Tay, N.W., Annan, N.C., Bhattamisra, S.K., Candasamy, M., 2019. Type 1 and 2 diabetes mellitus: A review on current treatment approach and gene therapy as potential intervention. *Diabetes Metab. Syndr.* 13, 364–372. <https://doi.org/10.1016/j.dsx.2018.10.008>.
- Tuccori, M., Filion, K.B., Yin, H., Yu, O.H., Platt, R.W., Azoulay, L., 2016. Pioglitazone use and risk of bladder cancer: Population based cohort study. *BMJ* 352, 1–8. <https://doi.org/10.1136/bmj.i1541>.
- Varga, T., Czimmerer, Z., Nagy, L., 2011. PPARs are a unique set of fatty acid regulated transcription factors controlling both lipid metabolism and inflammation. *Biochim. Biophys. Acta - Mol. Basis Dis.* 1812, 1007–1022. <https://doi.org/10.1016/j.bbadis.2011.02.014>.
- Yajima, K., Hirose, H., Fujita, H., Seto, Y., Fujita, H., Ukeda, K., Miyashita, K., Kawai, T., Yamamoto, Y., Ogawa, T., Yamada, T., Saruta, T., 2003. Combination therapy with PPAR γ and PPAR α agonists increases glucose-stimulated insulin secretion in db/db mice. *Am. J. Physiol. - Endocrinol. Metab.* 284, 966–971. <https://doi.org/10.1152/ajpendo.00149.2002>.
- Yang, W., Chen, X., Chen, M., Li, Y., Li, Q., Jiang, X., Yang, Y., Ling, W., 2017. Fish oil supplementation inhibits endoplasmic reticulum stress and improves insulin resistance: Involvement of AMP-activated protein kinase. *Food Funct.* 8, 1481–1493. <https://doi.org/10.1039/c6fo01841f>.
- Yang, Z., Wang, Y., Cheng, J., Shan, B., Wang, Y., Wang, R., 2019. Solid self-microemulsifying drug delivery system of Sophoraflavanone G : Prescription optimization and pharmacokinetic evaluation. *Eur. J. Pharm. Sci.* 136. <https://doi.org/10.1016/j.ejps.2019.06.007>
- Yki-Jarvinen, H., 2004. Drug therapy: Thiazolidinediones. *N. Engl. J. Med.* 351, 1106–1118. <https://doi.org/10.1056/NEJMra041001>.